RESEARCH ARTICLE | AUGUST 01 2024

# Periodic nonlinear dust-acoustic waves in multispecies dusty plasmas

Frank Verheest ; Carel P. Olivier



*Phys. Plasmas* 31, 083701 (2024)
https://doi.org/10.1063/5.0216920

Physics of Plasmas ARTICLE pubs.aip.org/aip/pop

# Periodic nonlinear dust-acoustic waves in multispecies dusty plasmas

Cite as: Phys. Plasmas **31**, 083701 (2024); doi: 10.1063/5.0216920
Submitted: 2 May 2024 · Accepted: 12 July 2024 ·
Published Online: 1 August 2024



Frank Verheest[1,2,a)] and Carel P. Olivier[3,b)]

## AFFILIATIONS

[1]Sterrenkundig Observatorium, Universiteit Gent, Krijgslaan 281, B-9000 Gent, Belgium
[2]School of Chemistry and Physics, University of KwaZulu-Natal, Scottsville, Pietermaritzburg 3209, South Africa
[3]Pure and Applied Analytics, School of Mathematical and Statistical Sciences, North-West University, Mahikeng Campus, Mmabatho 2745, South Africa

[a)]Author to whom correspondence should be addressed: frank.verheest@ugent.be
[b)]Electronic mail: carel.olivier@nwu.ac.za

## ABSTRACT

A pseudopotential analysis is presented for the propagation of nonlinear periodic dust-acoustic waves in a dusty plasma comprising cold negative dust, Boltzmann electrons, and Boltzmann or Cairns nonthermal positive ions, extending thus earlier treatments for ion-acoustic waves in electron–proton plasmas. The dusty plasma model where both electrons and ions are Boltzmann does not admit solitons, but works for nonlinear periodic waves. For consistency in the periodic case, two properties are required: conservation per cycle of species densities and that for very small amplitudes the waves resemble linear waves. The first property has to be imposed through a global perturbation of the undisturbed equilibrium, whereas the second property follows naturally from the formalism. After obtaining the general analytical methodology, a numerical analysis is discussed and illustrated with graphs for the electrostatic potential profile, the Sagdeev pseudopotential, the wave electric field, and the three different species densities, first for the Boltzmann and thereafter for the Cairns ions.





## I. INTRODUCTION

The interest in dusty plasmas comes from several sides, among which are important results from space observations by the Voyager missions of the Jovian and Cronian dust rings. These have drawn attention to the interaction between dust grains and plasmas. Notable examples are the radial spokes in the B ring[1] and the braiding of the F ring[2] of Saturn. Here phenomena have been observed that could not be explained by purely gravitational properties but required the presence of an electrically charged dust component. In this context, the physics of dusty plasmas concerns charged micrometer- to nanosized dust grains, which, if sufficiently numerous, can be treated as an additional fluid species that introduces a specific low-frequency component to a multispecies plasma.

The initial model for a dust-acoustic wave (DAW) is a bold transposition by Rao *et al.*[3] to the physics of dusty plasmas of the concept of an ion-acoustic wave,[4] first for linear and then solitary waves. To sustain an acoustic wave, at least two elements are needed: an inertial and a hot thermal species, in the earliest ion-acoustic models cold protons plus Boltzmann electrons. Because the charged dust grains are so much heavier than protons and electrons the obvious first model for DAWs consisted of cold negatively charged grains in the presence of proton and electron Boltzmann species, the inertia of which could be neglected compared to the dust grains.

The theoretical description is simple enough, consisting of the cold fluid dust continuity and momentum equations, and for the inertialess hot electrons and protons Boltzmann distributions.[5] The species densities are coupled by Poisson's equation for the electrostatic potential. This simple dust-acoustic dispersion model has been experimentally verified. Earlier discussions of collective effects in microplasmas by James and Vermeulen[6] using many-fluid models as in Verheest[7] were not addressing dusty plasmas as now understood.

All this quickly expanded into a whole new domain of the dusty plasma wave literature and has been summarized in various books, notably by Verheest[8] and Shukla and Mamun,[9] containing many relevant references. Coming in particular to the present paper, we will be guided by some properties known from the study of nonlinear solitary waves in dusty plasmas. The original model for the DAWs (cold negative dust and Boltzmann electrons and protons) claimed to admit

negative and positive polarity linear and nonlinear solitary DAWs,[3] although this has not been discussed in sufficient detail.

The parameter range of the negative polarity waves is limited by the infinite dust compression, the positive polarity waves being restricted by encountering a double layer. A worked-out example of nonthermal distributions is based on the so-called Cairns distribution,[10] but kappa[11,12] or later Tsallis distributions[13,14] might presumably also do the trick.

There is an important distinction between nonlinear solitary vs periodic waves and the perturbations of the undisturbed equilibrium needed to generate them. As the soliton profile has a finite area under the curve for the electrostatic potential in a co-moving frame, the energy and related quantities are finite, thus the perturbation necessary to excite the wave can be a local one, confined to a small area of the spatial domain. For nonlinear periodic waves, however, the species densities should be conserved over one cycle, because otherwise an excess or loss of density per cycle becomes, over an infinity of cycles, an infinite excess or loss, which is physically unacceptable. This density conservation requires a global perturbation, even though the relevant changes in the maximum and minimum amplitudes might be small.

In this respect, most of the extant literature on nonlinear periodic waves is not correct and does not conserve the species densities. We will only cite here the deficient papers concerning themselves with DAWs.[15–20] It is only in four recent papers that the picture has been corrected,[21–24] all for simple proton–electron plasmas, not yet for DAWs. Another desirable phenomenon is that the small amplitude limit of the nonlinear periodic waves resembles very much what one would obtain from a linearized description in terms of sine or cosine modes. That seems to obtain from the mathematical and numerical analysis without having to be imposed from the outset.

For the DAWs, we will follow the model discussed by Verheest and Pillay[25] for solitons in plasmas with negative dust, where the electrons are Boltzmann but the protons have a Cairns nonthermal density distribution, which allowed positive polarity solitons. Using this composition for obtaining nonlinear periodic DAWS needs a careful attention to the boundary conditions and to the introduction of restrictions leading to density conservation. Interchanging the model to positive dust, amounts essentially to a mathematical interchange of the polarities in the formalism but engenders no specific difficulties.[26]

In particular and in contrast with our earlier efforts for electron-ion plasmas, there are now three densities to be separately conserved: for the cold dust grains, Boltzmann electrons, and nonthermal Cairns protons. This will impact on the global initial perturbation, together with the occurrence of several additional compositional parameters, rendering the numerical evaluation rather more complicated. As seen in our earlier papers, it is relatively easy to establish existence domains for periodic nonlinear waves, as long as the wave velocity and obliquity parameters are adequately chosen inside the appropriate domains.

Periodic electric field signals have been reported in many regions of Earth's magnetosphere (see, for example, Pickett *et al.*,[27] Rufai,[28] Singh *et al.*[29] and references therein), and therefore, we will specifically address also the electric field profiles in the numerical discussions. In space observations, electric field profiles are easier to record than electrostatic potentials or species densities.

The paper is organized as follows. After the introduction, we give in Sec. II the basic Sagdeev analysis, which is then numerically discussed in Sec. III. Our conclusions are summarized in Sec. IV.

## II. BASIC SAGDEEV ANALYSIS

We consider the model of a dusty plasma consisting of cold, singly charged negative dust, Boltzmann electrons, and Cairns nonthermal protons.

Following the Cairns distribution,[10,25] the normalized proton density $n_i$ is given at the macroscopic level by

$$n_i = (1 + \beta\varphi + \beta\varphi^2)\exp[-\varphi], \tag{1}$$

where $\varphi$ is the electrostatic potential of the wave or structure, normalized to $\kappa T_i/e$, with $\kappa$ being Boltzmann's constant. Here, $T_i$ is the temperature the ions would have in the absence of nonthermal effects. The latter are characterized by a parameter $\beta$.

In common with many descriptions of dusty plasma waves, the very mobile electrons have been assumed Boltzmann distributed, in normalized form,

$$n_e = (1 - f)\exp[\tau\varphi], \tag{2}$$

where $\tau = T_i/T_e$ is the ion-to-electron temperature ratio, with electron temperature $T_e$. Here, $f$ is the fraction of the negative charge density taken up by the dust relative to the positively charged ions at equilibrium; hence, $(1 - f)$ represents the equilibrium electron charged density fraction.

For one-dimensional structures, the cold, negative, and singly charged dust is described by the equations of continuity,

$$\frac{\partial n_d}{\partial t} + \frac{\partial}{\partial x}(n_d u_d) = 0, \tag{3}$$

and momentum,

$$\frac{\partial u_d}{\partial t} + u_d\frac{\partial u_d}{\partial x} = \frac{\partial \varphi}{\partial x}. \tag{4}$$

These nondimensional equations are written in standard normalized units.[25] The model of singly charged negative dust is easily extended to other charge numbers by adapting the normalization.

The basic equations are coupled by the Poisson equation

$$\frac{\partial^2\varphi}{\partial x^2} + n_i - n_e - n_d = 0. \tag{5}$$

In what follows, we will work in a frame co-moving with the structure, by introducing

$$\xi = x - Vt, \tag{6}$$

where $V$ is the velocity of the nonlinear wave.

To present the conservation laws that the solutions have to obey, we start by integrating (5), written in terms of $\xi$, over one wavelength $L$ (to be defined below) of the periodic structure. This yields

$$\int_0^L (n_i - n_e - n_d)d\xi = -\int_0^L \frac{d^2\varphi}{d\xi^2}d\xi = \frac{d\varphi}{d\xi}\Big|_{\xi=0} - \frac{d\varphi}{d\xi}\Big|_{\xi=L} = 0, \tag{7}$$

because of the periodicity of the $\varphi$ profile after one wavelength. Hence, there is conservation of the *global* density over one period, written as

$$\int_0^L n_i d\xi = \int_0^L (n_e + n_d)d\xi. \tag{8}$$

As noted before,[23] this conservation law is not dependent on the specific species descriptions. The unperturbed equilibrium densities

are $n_i = 1$, $n_e = 1 - f$ and $n_d = f$ for all $\xi$ and would give $L$, $(1-f)L$ and $fL$, respectively, when integrated over one wavelength $L$. We thus impose the conservation of species number densities through

$$\int_0^L (n_i - 1) d\xi = 0, \tag{9}$$

$$\int_0^L [n_e - (1-f)] d\xi = 0, \tag{10}$$

$$\int_0^L (n_d - f) d\xi = 0. \tag{11}$$

Because $d\varphi/d\xi = 0$ at the minimum and maximum values $\varphi = \varphi_{min}$ and $\varphi = \varphi_{max}$, there necessarily is an intermediate value where the tangent $d\varphi/d\xi$ reaches a positive maximum $\alpha = d\varphi/d\xi|_{\xi=0} > 0$. This inflection point has been taken as the origin of the $\xi$-axis, which can be done without loss of generality. Consequently, $d^2\varphi/d\xi^2|_{\xi=0} = 0$. Furthermore, we denote the function values at the inflection point as $n_i(0) = \gamma_i$, $n_e(0) = \gamma_e$, $n_d(0) = \gamma_d$, $u_d(0) = 0$ and $\varphi(0) = 0$, to be further elucidated and discussed below. The choice $\varphi(0) = 0$ then ensures $\varphi_{min} < 0$ and $\varphi_{max} > 0$, an essential prerequisite to ensure the possibility of charge density conservation.

For numerical simplicity, we take here $u_d(0) = 0$ rather than $u_d(0) = u_0$ as in earlier papers, where the latter choice allowed for the additional conservation of ion flux that then determined $u_0$ uniquely. However, $u_0 \neq 0$ amounts to a Doppler shift on $V$, and but for that change the mathematics are essentially the same. For the multispecies model discussed here, there are already enough additional parameters to consider, and we have thus preferred to leave $u_0$ out of the analytics. Should the explicit conservation of dust flux be desired, the analytical modifications are straightforward to implement.[23]

We rewrite (3) and (4) in terms of $\xi$ with the help of Eq. (6) and integrate the resulting expressions with respect to $\xi$, starting not from the undisturbed quantities but from a global perturbation for periodic structures. Eliminating $u_d$ between the two expressions thus obtained leads to

$$n_d = \frac{f\gamma_d}{\sqrt{1 + \frac{2\varphi}{V^2}}} \tag{12}$$

with the square root form which is typical for cold plasma species. When Eq. (12) is inserted into Eq. (11), the factor $f$ falls away and the conservation of dust density becomes

$$\int_0^L \left( \frac{\gamma_d}{\sqrt{1 + \frac{2\varphi}{V^2}}} - 1 \right) d\xi = 0. \tag{13}$$

Introducing the factors $\gamma_i$ and $\gamma_e$ in the expressions (1) and (2) yields

$$n_i = \gamma_i (1 + \beta\varphi + \beta\varphi^2) \exp[-\varphi], \tag{14}$$

$$n_e = (1-f)\gamma_e \exp[\tau\varphi]. \tag{15}$$

For the numerical computation later on, analogous as occurred for the charged dust, the conditions (9) and (10) become

$$\int_0^L \{\gamma_i (1 + \beta\varphi + \beta\varphi^2) \exp[-\varphi] - 1\} d\xi = 0, \tag{16}$$

$$\int_0^L \{\gamma_e \exp[\tau\varphi] - 1\} d\xi = 0, \tag{17}$$

so that also the factor $(1-f)$ is canceled in the electron density condition.

Because the initial perturbation must obey (5), the three density parameters are linked,

$$\gamma_i = (1-f)\gamma_e + f\gamma_d, \tag{18}$$

a significant change in the methodology, where for electron–ion plasmas one $\gamma$ factor sufficed.

We have investigated what happens if one were to assume that $\gamma_e = \gamma_d$ (so that also $\gamma_i$ became equal), but the numerical computation showed only one of the species densities to be conserved. There are therefore two distinct values $\gamma$ to consider, $\gamma_e$ and $\gamma_d$. In this way, (13) and (17) can be worked out for the conservation of the electron and dust densities per cycle, respectively. According to the theoretical analysis, (8) and (18) should then lead to Eq. (16) being obeyed and the ion density also conserved. This will be used later as a check on the consistency of the numerics, when Eq. (16) is computed separately.

Poisson's equation thus becomes

$$\frac{d^2\varphi}{d\xi^2} + \gamma_i (1 + \beta\varphi + \beta\varphi^2) \exp[-\varphi] - (1-f)\gamma_e \exp[\tau\varphi] - \frac{f\gamma_d}{\sqrt{1 + \frac{2\varphi}{V^2}}} = 0. \tag{19}$$

After multiplying this by $d\varphi/d\xi$, we can integrate with respect to $\xi$ and obtain an energy-like integral,

$$\frac{1}{2}\left(\frac{d\varphi}{d\xi}\right)^2 + S(\varphi) = 0. \tag{20}$$

$S(\varphi)$ is the Sagdeev pseudopotential,[30] here

$$S(\varphi) = \gamma_i \{1 + 3\beta - (1 + 3\beta + 3\beta\varphi + \beta\varphi^2) \exp[-\varphi]\} + \frac{(1-f)\gamma_e}{\tau}(1 - \exp[\tau\varphi]) + f\gamma_d V^2 \left(1 - \sqrt{1 + \frac{2\varphi}{V^2}}\right) - \frac{1}{2}\alpha^2, \tag{21}$$

the behavior of which will have to be studied as we vary the compositional model parameters $f$, $\beta$, and $\tau$. The structure parameters, $\alpha$ (inclination at inflection point, later measure for the amplitude) and $V$ (velocity), will then determine the properties of the periodic nonlinear structures. For ease of subsequent notation, we introduce

$$A(\varphi) = \gamma_i \{1 + 3\beta - (1 + 3\beta + 3\beta\varphi + \beta\varphi^2) \exp[-\varphi]\} + \frac{(1-f)\gamma_e}{\tau}(1 - \exp[\tau\varphi]). \tag{22}$$

One can easily show that $S(\varphi) \to -\infty$ for $\varphi \to +\infty$, so that positive roots, if they occur, must occur in pairs. When $V$ is sufficiently increased, the pair closest to the origin becomes a double root. $S(\varphi)$ does not have enough flexibility for positive roots beyond that and the range of positive roots thus ends at the double layer. The double layer equations are derived from Eq. (21) and written for $\varphi = \varphi_{dl}$ as

$$S(\varphi_{dl}) = A(\varphi_{dl}) + f\gamma_d V^2\left(1 - \sqrt{1 + \frac{2\varphi_{dl}}{V^2}}\right) - \frac{1}{2}\alpha^2 = 0, \quad (23)$$

and the derivative

$$S'(\varphi_{dl}) = A'(\varphi_{dl}) - \frac{f\gamma_d}{\sqrt{1 + \frac{2\varphi_{dl}}{V^2}}} = 0. \quad (24)$$

Here, the prime denotes derivatives of $S(\varphi)$ and $A(\varphi)$ with respect to $\varphi$. Now Eq. (24) is solved for $V^2$ as a function of $\varphi_{dl}$,

$$V^2 = \frac{2\varphi_{dl}A'(\varphi_{dl})^2}{f^2\gamma_d^2 - A'(\varphi_{dl})^2}, \quad (25)$$

and substituted in Eq. (23). This allows us to write $\alpha^2$ as

$$\alpha^2 = A(\varphi_{dl}) - \frac{2f\gamma_d\varphi_{dl}A'(\varphi_{dl})}{f\gamma_d + A'(\varphi_{dl})}. \quad (26)$$

The parametric plotting of $V$ as a function of $\alpha$ yields an upper curve, whereby $\varphi_{dl}$ serves as a kind of dummy variable. Above this curve, there are no longer double layers to be found and hence also no positive roots, so that periodic nonlinear waves cannot exist.

We can also introduce the limit

$$\varphi_{lim} = -\frac{V^2}{2}, \quad (27)$$

obtained from Eq. (12) at infinite dust compression and then $S(\varphi_{lim}) = 0$ yields the plot of $\alpha$ as a function of $V$ for the lower, dashed blue curve in the existence diagram, as illustrated below in Fig. 1.

At this stage, we remark that for $\alpha = 0$, not only does the amplitude go to zero (constant equilibrium solution), but the Sagdeev pseudopotential recovers the expression used to discuss solitons, but derived under a different set of boundary conditions.[25] Indeed, for $\alpha = 0$, the origin of the reference frame for the Sagdeev pseudopotential becomes an unstable maximum, precisely what is needed to obtain solitons. In that case, we know that negative polarity solitons occur until the dust compression limit is reached. Positive polarity solitons are limited by the occurrence of positive double layers, requiring a nonzero minimal degree of nonthermality of the proton plasma component. The interpretation of this result is that the very early plasma model for DAWs, cold negative dust and Boltzmann electrons and ions, can only give rise to negative polarity solitons.

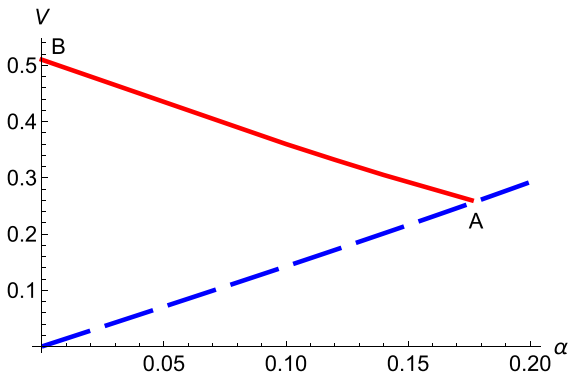


**FIG. 1.** Limiting curves for cold dust, Boltzmann electrons and ions, with average parameters $\beta = 0, f = 0.5, \tau = 1, \gamma_i = \gamma_e = \gamma_d = 1$. The acceptable choices of $\{\alpha, V\}$ lie above the blue dashed curve expressing the cold dust compression limit and below the red solid curve indicating the positive double layer limit.

However, we are investigating nonlinear periodic DAWs and will show in Sec. III that even in the case of Boltzmann ions ($\beta = 0$) such waves are possible, keeping in mind that for periodic waves in the Sagdeev formalism the pseudopotential needs to have at least one positive and one negative root, otherwise species densities cannot be conserved. Perhaps unexpectedly, this is an interesting and rather unusual model, because although positive nonlinear solitary waves cannot be sustained, nonlinear periodic waves can!

We will also treat the case of $\beta \neq 0$, but because of the many parameters to be considered and discussed, we will show how to determine the existence regions in parameter space but confine ourselves to a few proof-of-principle worked-out examples. We have indeed seen in our earlier efforts[23,24] for ion-acoustic waves in electron–ion plasmas that the parametric discussion quickly generates a series of similar looking figures and numerical tables, without really enlarging our physical understanding.

## III. NUMERICAL ANALYSIS

### A. Model with Boltzmann electrons and ions, plus negative dust

To start the numerical analysis, we plot the two limiting curves in $\{\alpha, V\}$ space, as shown in Fig. 1. The blue dashed curve starting from $V = 0$ reflects the dust density compression limit, whereas the solid red curve starting from the highest $V$ for $\alpha = 0$ indicates the occurrence of positive double layers. Outside the triangular region no solutions can exist. The highest $V$ corresponds to the correct acoustic velocity $c_{da}$, and because $V < c_{da}$ for admissible $V$, the periodic nonlinear DAWs are subsonic, whereas at $\alpha = 0$, we are in the soliton regime and those are known to be supersonic. Small changes in the different $\gamma$ away from 1 will affect the existence triangle, but for simplicity we have used $\gamma_e = \gamma_d = \gamma_i = 1$ to produce Fig. 1.

The idea is to pick a pair of $\{\alpha, V\}$ values inside the existence triangle, for chosen compositional parameters $f$ and $\tau$, and then find the corresponding $\gamma_e, \gamma_d, \gamma_i$ to conserve the species densities. For Boltzmann ions, $\beta = 0$. We thus compute in Table I for various $f$ and $\tau$ combinations values for $\alpha$ and $V$ which can produce periodic nonlinear DAWs.

For $f = 0.1, 0.5, 0.9$, there is more and more dust, which cannot be totally absent because without the dust there is no inertial species to sustain the waves, hence $f \neq 0$. On the other hand, $f = 1$ means that all electrons are accreted to the dust, and a two-component plasma composed of negative cold dust and Boltzmann (or Cairns) ions is, up to a change in polarities and charge signs, mathematically the same as the case of positive cold ions and Boltzmann or Cairns electrons treated in our earlier Sagdeev papers.[23,24]

Typical values of $\tau = 0.1, 1, 10$ indicate that $T_e = 10, 1, 0.1$ times $T_i$, respectively, so increases in $\tau$ are interpreted as decreases in $T_e$, given that the yardstick for the temperatures has been chosen as $T_i$.

We know from previous papers[23,24] that any such pair $\{\alpha, V\}$ will generate graphs which look qualitatively similar, only differing quantitatively. There is not really a great need to produce all these graphs; they will not add much to our physical understanding but require some effort to arrive at the correct $\gamma$ factors to ensure density conservation for the three species.

**TABLE I.** Typical $\alpha$ and $V$ values for chosen $f$ and $\tau$. The positive ions are assumed Boltzmann ($\beta = 0$) and the density scaling parameters are for simplicity $\gamma_i = \gamma_e = \gamma_d = 1$. The numbers in the third column correspond to the highest $\alpha$ at the top $A$ of the existence triangle, with medium values of $V$. The numbers in the fifth column correspond to small $\alpha$ but reaching the highest $V$ at the point $B$, along the ordinate in $\{\alpha, V\}$ space. Blanks indicate that the parameter ranges are already small and little different from the numbers given on the same line in the preceding set.

| $f$ | $\tau$ | $\alpha$ | $V$ | $\alpha$ | $V$ |
|---|---|---|---|---|---|
| 0.1 | 0.1 | 0.04 | 0.14 | | |
| 0.1 | 1 | 0.03 | 0.10 | | |
| 0.1 | 10 | 0.01 | 0.05 | | |
| 0.5 | 0.1 | 0.21 | 0.33 | 0.10 | 0.47 |
| 0.5 | 1 | 0.17 | 0.26 | 0.10 | 0.36 |
| 0.5 | 10 | 0.08 | 0.12 | | |
| 0.9 | 0.1 | 0.40 | 0.44 | 0.10 | 0.77 |
| 0.9 | 1 | 0.39 | 0.43 | 0.10 | 0.72 |
| 0.9 | 10 | 0.22 | 0.25 | 0.10 | 0.41 |

From Table I, we see that at fixed $f$, the existence region (as in Fig. 1) shrinks when $\tau$ is increased. Therefore, we chose smaller parameters for larger $\tau$ in Table I. An increase in $\tau$ means a decrease in both parameters $\{\alpha, V\}$, but an increase in $\tau$ signifies a decrease in $T_e/T_i$. At fixed $\tau$, we note that the parameters $\{\alpha, V\}$ increase with $f$. This is for Boltzmann ions ($\beta = 0$), but we will see later, in Table II, that for Cairns ions (e.g., $\beta = 0.5$) the same trends hold, but at higher values for $\{\alpha, V\}$, owing to the nonthermality in the ion component.

After this general discussion, we will pick a specific plasma model with the parameters $\beta = 0, f = 0.5, \tau = 1$ and wave values $\alpha = 0.15, V = 0.26$ within the existence region. The compositional parameters have been taken for typical values, $f = 0.5$ and $\tau = 1$, as soliton results have indicated that variations here usually produce little quantitative changes. For those parameters, the density correction factors turn out to be $\gamma_d = 1.148\,756\,9$, $\gamma_e = 0.950\,844\,8$, and $\gamma_i = 1.049\,800\,8$. These are determined by the numerical integration of Poisson's equation (19) under the accompanying assessment of the conservation laws (13), (16), and (17). Remarkably, although (18) has been used in the numerical algorithm, the correct determination of $\gamma_d$ and $\gamma_e$ from Eqs. (13) and (17), respectively, also annuls (16), serving thus as a useful check on the numerics. The numerical precision on the various density parameters $\gamma$ is of order $10^{-7}$.

We show in Fig. 2(a), the electrostatic profile of the periodic nonlinear DAW, for typical compositional parameters $f = 0.5, \tau = 1$, wave properties $V = 0.26, \alpha = 0.15$, and inflection point densities $\gamma_d = 1.148\,756\,9$, $\gamma_e = 0.950\,844\,8$, $\gamma_i = 1.049\,800\,8$, needed to conserve the species densities. From the profile in Fig. 2(a), we can deduce the wavelength $L = \xi_{max} - \xi_{min} = 2.954\,329$, where $\xi_{max}$ is the smallest of the positive roots and $\xi_{min}$ the largest of the negative roots of the Sagdeev potential. In addition, as we are not dealing with linear waves, we define $\Phi = \varphi_{max} - \varphi_{min} = 0.130\,615$ as a measure for the amplitude and $\varphi_{min}, \varphi_{max}$ have been introduced already below (11).

We also show in Fig. 2(b), the corresponding Sagdeev pseudopotential with its three roots, one negative at $\varphi_{min}$ and two positive, of which the first is $\varphi_{max}$ and the second has no physical meaning, as it cannot be reached from the undisturbed values. The quite spiky electric field is shown in Fig. 2(c). Similar profiles have been observed in many regions of Earth's magnetosphere (see, for example, Pickett *et al.*,[27] Rufai,[28] Singh *et al.*[29] and references therein).

Finally, the three species' densities are combined in Fig. 3, with the ion density indicated in blue, the electron density in red, and the dust density in green. It is remarked that the dust density compression is severely spiked (the top part of this spike is truncated for visual clarity), compensated by a longer but shallower rarefaction.

**TABLE II.** Typical $\alpha$ and $V$ values for chosen $f$ and $\tau$. The positive ions are Cairns distributed and a high nonthermality is taken as $\beta = 0.5$. The density scaling parameters are for simplicity $\gamma_i = \gamma_e = \gamma_d = 1$. The numbers in the third column correspond to the highest $\alpha$ at the top of the existence triangle, with medium values of $V$. The numbers in the fifth column correspond to small $\alpha$ but reaching the highest $V$, along the ordinate in $\{\alpha, V\}$ space. Blanks here indicate that the parameter ranges are already small and little different from the numbers given in the preceding set on the same line.

| $f$ | $\tau$ | $\alpha$ | $V$ | $\alpha$ | $V$ |
|---|---|---|---|---|---|
| 0.1 | 0.1 | 0.05 | 0.20 | | |
| 0.1 | 1 | 0.03 | 0.13 | | |
| 0.1 | 10 | 0.01 | 0.05 | | |
| 0.5 | 0.1 | 0.34 | 0.53 | 0.10 | 0.79 |
| 0.5 | 1 | 0.21 | 0.32 | 0.10 | 0.48 |
| 0.5 | 10 | 0.08 | 0.13 | | |
| 0.9 | 0.1 | 0.73 | 0.84 | 0.10 | 1.33 |
| 0.9 | 1 | 0.55 | 0.65 | 0.10 | 1.10 |
| 0.9 | 10 | 0.23 | 0.27 | 0.10 | 0.46 |

## B. Model with Boltzmann electrons, Cairns ions and negative dust

Now we deal with Cairns instead of Boltzmann ions, and choose $\beta = 0.5$ as appropriate for strong nonthermality, as it is near but smaller than the upper limit $\beta = 4/7 \simeq 0.57$ beyond which the underlying microscopic Cairns distribution starts to develop nonmonotonic beam-like characteristics.[25] The existence region is shown in Fig. 4, for average parameters $\beta = 0.5, f = 0.5, \tau = 1$, and simplified $\gamma_i = \gamma_e = \gamma_d = 1$.

Note that the ranges in $V$ and $\alpha$ are now larger than for the Boltzmann ions shown in Fig. 1, owing to the effects of nonthermality.

We can thus generate Table II, with an arrangement similar to that in Table I. A comparison between the two tables confirms that the $\{\alpha, V\}$ existence region increases with the nonthermal parameter $\beta$.

For the illustration of a typical example, we pick compositional parameters $\beta = 0.5, f = 0.5, \tau = 1$, wave parameters $\alpha = 0.2, V = 0.3$, and then the density conditions yield $\gamma_d = 1.153\,078\,7, \gamma_e = 0.920\,749\,2, \gamma_i = 1.036\,914\,0$. The wavelength is $L = 3.335\,177$ and the measure for the amplitude $\Phi = 0.197\,049$. Due to the nonthermality, these values are larger than the corresponding values obtained for the Boltzmann ion model.

For these values, the results are shown in Fig. 5 for the electrostatic periodic profile, the Sagdeev pseudopotential, and the wave electric field and in Fig. 6 for the species densities. The

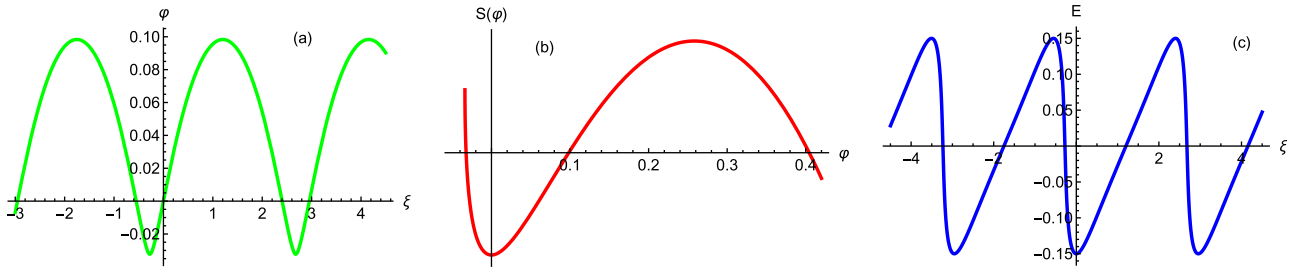


**FIG. 2.** Typical (a) profile, (b) Sagdeev pseudopotential and (c) electric field, for Boltzmann ions and $f = 0.5, V = 0.26, \alpha = 0.15, \tau = 1$, and $\gamma_d = 1.148\,756\,9$, $\gamma_e = 0.950\,844\,8$, $\gamma_i = 1.049\,800\,8$, conserving species densities.

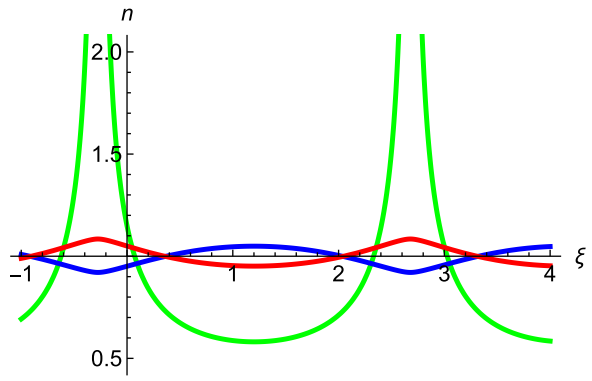


**FIG. 3.** Typical densities for Boltzmann ion model and the same parameters as in Fig. 2. The color coding for the densities are blue for the ions, red for the electrons, and green for the dust. For graphical clarity, the dust density compression is only shown to $n_d = 2$, but reaches up to 5.4.

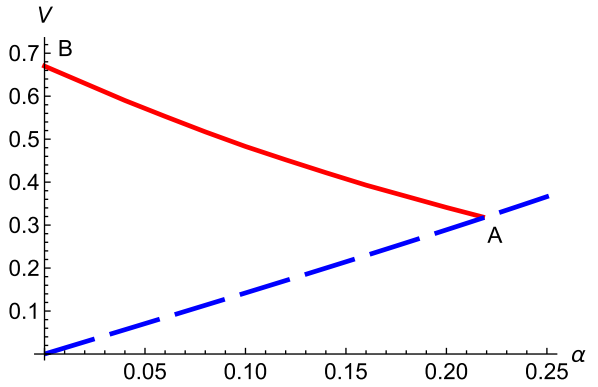


**FIG. 4.** Limiting curves for cold dust, Boltzmann electrons and Cairns ions, with average parameters $\beta = 0.5, f = 0.5, \tau = 1, \gamma_i = \gamma_e = \gamma_d = 1$. The acceptable choices of $\{\alpha, V\}$ lie above the blue dashed curve expressing the cold dust compression limit and below the red solid curve indicating the positive double layer limit.

qualitative agreement with the corresponding results for $\beta = 0$ is obvious.

Note that for graphical clarity the serious dust density compression has not been show above $n_d = 2$, because otherwise the subtleties in the electron and ion densities are obliterated. In reality, $n_d$ at maximum compression goes up to 11.45. This high level of compression is indicative of its close proximity to the infinite compression limit that acts as the upper bound for $\alpha$.

### C. Small amplitude quasi-linear waves

There is obviously a clear link between $\alpha$ and wave amplitude $\Phi$, $\alpha$ to be found on ordinate axis. Note the differences in scale between the two parts of Fig. 7, due to the nonthermality induced by the Cairns model, leading to larger velocities and amplitudes. For smaller wave amplitudes, the hodographs tend to the ellipses one gets for linear waves, having a profile $\varphi \propto \sin \xi$.

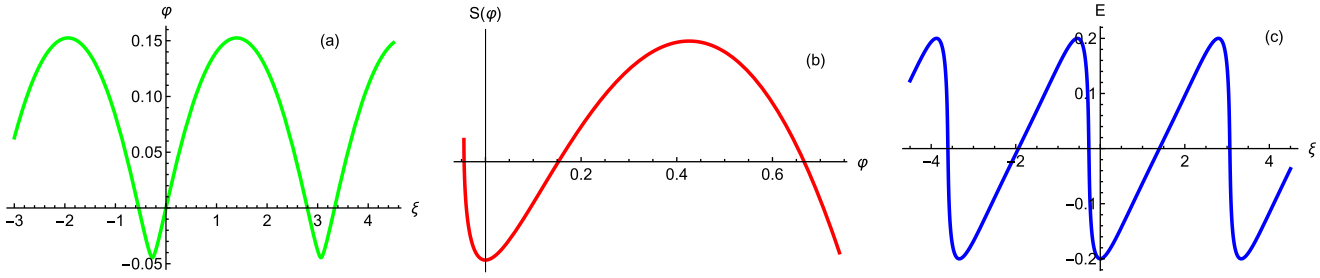


**FIG. 5.** Typical (a) profile, (b) Sagdeev pseudopotential, and (c) electric field, for Cairns ions and $\beta = 0.5, f = 0.5, V = 0.3, \alpha = 0.2, \tau = 1$, and $\gamma_d = 1.153\,078\,7$, $\gamma_e = 0.920\,749\,2$, $\gamma_i = 1.036\,914\,0$, conserving species densities.

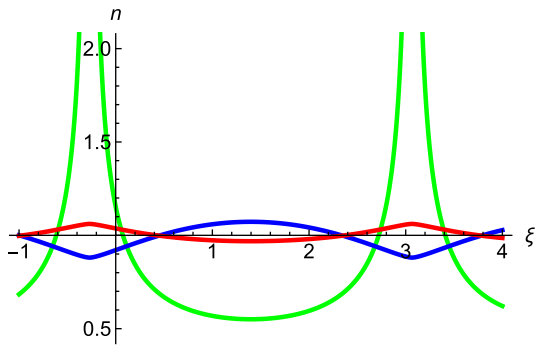


**FIG. 6.** Typical densities for Cairns ion model and the same parameters as in Fig. 5. The color coding for the densities are blue for the ions, red for the electrons, and green for the dust. The range in upper amplitudes has for graphical clarity been topped at $n_d = 2$. In reality, it goes up to $n_d = 11.45$.

Both the Boltzmann and Cairns distributions for the positive ions have been further compared in Table III.

We illustrate the quasi-linear, almost cosinusoidal character also for the electric field in Fig. 8.

## IV. SUMMARY

We have applied an analogous Sagdeev pseudopotential formalism to the description of nonlinear periodic dust-acoustic waves that was before used for the simpler model of nonlinear periodic ion-acoustic modes.[23,24] The fundamental difference is that with more species than just electrons and positive ions one has to introduce more density parameters in the initial global perturbations in order to conserve the individual species densities per cycle of the nonlinear periodic wave. For the usual dust-acoustic wave model, there are three species, and this requires two density parameters instead of one, given that there is always a global relation between the species densities implied in Poisson's equation. All this renders the analytical and the numerical analyses more complicated, but surmountable.

Nevertheless, the same salient characteristics were imposed or obtained as for ion-acoustic models. These are (a) the conservation of species densities per cycle and (b) mimicking linear wave properties for very small obliquity. Characteristic (a) is an analytical requirement that has to be imposed to arrive at a physically correct description, whereas on the other hand characteristic (b) follows from the numerical analysis at small amplitudes. In erroneous treatments, the small amplitude limits cannot be connected with the undisturbed conditions

**TABLE III.** $\beta, \alpha, V$ and density scaling parameters $\gamma_d, \gamma_e, \gamma_i$, for typical $f = 0.5$ and $\tau = 1$. The positive ions are either Boltzmann ($\beta = 0$) or Cairns distributed at high nonthermality ($\beta = 0.5$).

| $\beta$ | $\alpha$ | $V$ | $\gamma_d$ | $\gamma_e$ | $\gamma_i$ |
|---|---|---|---|---|---|
| 0 | 0.15 | 0.26 | 1.148 756 9 | 0.950 844 8 | 1.049 800 8 |
| 0 | 0.10 | 0.26 | 1.068 274 5 | 0.977 039 2 | 1.022 656 8 |
| 0 | 0.05 | 0.26 | 1.017 437 0 | 0.994 070 2 | 1.005 753 6 |
| 0 | 0.01 | 0.26 | 1.000 702 5 | 0.999 760 2 | 1.000 231 4 |
| 0.5 | 0.20 | 0.30 | 1.153 078 7 | 0.920 749 2 | 1.036 914 0 |
| 0.5 | 0.10 | 0.30 | 1.042 289 8 | 0.979 074 8 | 1.010 182 3 |
| 0.5 | 0.05 | 0.30 | 1.010 878 5 | 0.994 357 8 | 1.002 618 2 |
| 0.5 | 0.01 | 0.30 | 1.000 439 3 | 0.999 772 1 | 1.000 105 7 |

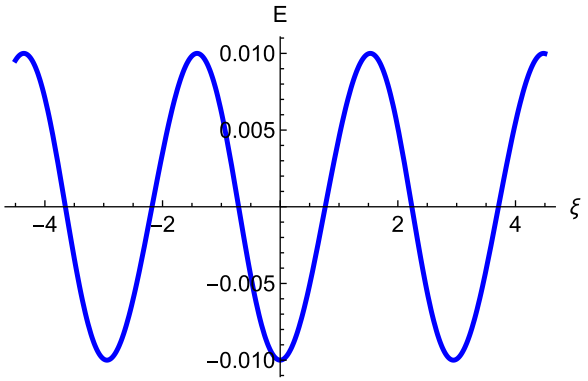


**FIG. 8.** Typical electric field, for Cairns ions and $\beta = 0.5$, $f = 0.5, V = 0.3$, $\alpha = 0.01, \tau = 1$, and $\gamma_d = 1.000\,439\,3$, $\gamma_e = 0.0.999\,772\,1$, $\gamma_i = 1.000\,105\,7$, showing the quasi-linear profile of the electric field, far from the more sawtooth ones found at larger amplitudes.

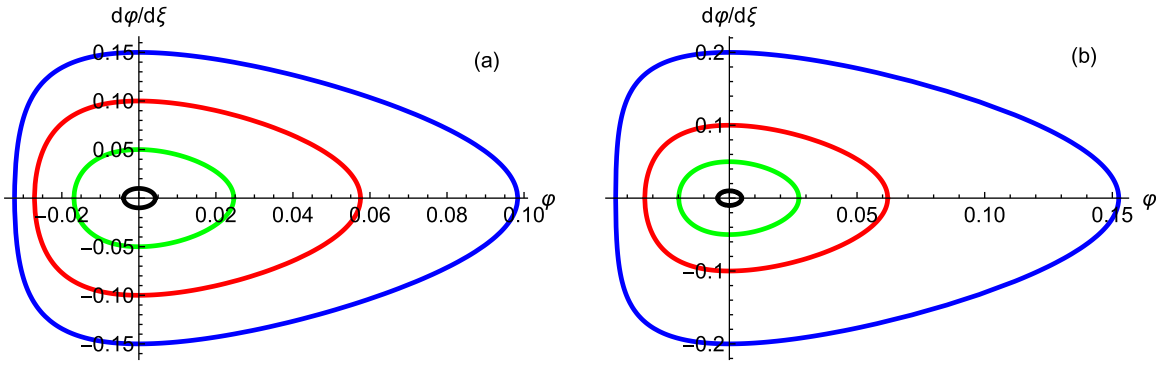


**FIG. 7.** Typical hodographs for (a) the Boltzmann ion model at $V = 0.26$ and decreasing $\alpha = 0.15$ (blue), 0.10 (red), 0.05 (green), and 0.01 (black), and (b) Cairns ion model, at $\beta = 0.5$, $V = 0.3$ and decreasing $\alpha = 0.20$ (blue), 0.10 (red), 0.05 (green), and 0.01 (black). Other parameters are listed in Table III.

and, thus, leave a conceptual gap between linear and nonlinear periodic waves which is physically not understandable.

Finally, it is obvious that even more sophisticated plasma models can be treated, by establishing proper extensions of the Sagdeev formalism for nonlinear periodic waves. The repetitivity of the various figures obtained in earlier papers and here illustrates this very well. However, it is not our intention to add a spate of more papers on this topic, as has been the case for the description of solitons in various multispecies plasmas. The essential difference with the soliton theory is that for periodic nonlinear modes, one needs precise global rather than local initial perturbations. That might render solitons easier to generate in nature than really periodic modes. This is rather peculiar, given that after the original observations of solitons on shallow water surfaces, it took quite some time before they were recognized as different from the ubiquitous linear wave pictures.

## ACKNOWLEDGMENTS

This work is based on research supported in part by the National Research Foundation of South Africa (Grant No. 145712).

## AUTHOR DECLARATIONS

### Conflict of Interest

The authors have no conflicts to disclose.

### Author Contributions

**Frank Verheest:** Conceptualization (equal); Formal analysis (equal); Writing – original draft (lead); Writing – review & editing (equal). **Carel Petrus Olivier:** Conceptualization (equal); Formal analysis (equal); Writing – original draft (supporting); Writing – review & editing (equal).

## DATA AVAILABILITY

Data sharing is not applicable to this article as no new data were created or analyzed in this study.

## REFERENCES

[1]B. A. Smith, L. Soderblom, R. Beebe, J. Boyce, G. Briggs, A. Bunker, S. A. Collins, C. J. Hansen, T. V. Johnson, J. L. Mitchell, R. J. Terrile, M. Carr, A. F. Cook II, J. Cuzzi, J. B. Pollack, G. E. Danielson, A. Ingersoll, M. E. Davies, G. E. Hunt, H. Masursky, E. Shoemaker, D. Morrison, T. Owen, C. Sagan, J. Veverka, R. Strom, and V. E. Suomi, "Encounter with Saturn: Voyager 1 imaging science results," Science **212**, 163–191 (1981).

[2]B. A. Smith, L. Soderblom, R. Batson, P. Bridges, J. Inge, H. Masursky, E. Shoemaker, R. Beebe, J. Boyce, G. Briggs, A. Bunker, S. A. Collins, C. J. Hansen, T. V. Johnson, J. L. Mitchell, R. J. Terrile, A. F. Cook II, J. Cuzzi, J. B. Pollack, G. E. Danielson, A. Ingersoll, M. E. Davies, G. E. Hunt, D. Morrison, T. Owen, C. Sagan, J. Veverka, R. Strom, and V. E. Suomi, "A new look at the Saturn system: The Voyager 2 images," Science **215**, 504–537 (1982).

[3]N. N. Rao, P. K. Shukla, and M. Y. Yu, "Dust-acoustic waves in dusty plasmas," Planet. Space Sci. **38**, 543–546 (1990).

[4]H. Washimi and T. Taniuti, "Propagation of ion-acoustic solitary waves of small amplitude," Phys. Rev. Lett. **17**, 996–998 (1966).

[5]F. Verheest, "Nonlinear dust-acoustic waves in multispecies dusty plasmas," Planet. Space Sci. **40**, 1–6 (1992).

[6]C. R. James and F. Vermeulen, "A microparticle plasma," Can. J. Phys. **46**, 855–863 (1968).

[7]F. Verheest, "General dispersion relations for linear waves in multicomponent plasmas," Physica **34**, 17–35 (1967).

[8]F. Verheest, *Waves in Dusty Space Plasmas* (Kluwer Academic Publishers, Dordrecht, 2000).

[9]P. K. Shukla and A. A. Mamun, *Introduction to Dusty Plasma Physics* (Routledge, Taylor & Francis, London, 2001).

[10]R. A. Cairns, A. A. Mamun, R. Bingham, R. Boström, R. O. Dendy, C. M. C. Nairn, and P. K. Shukla, "Electrostatic solitary structures in non-thermal plasmas," Geophys. Res. Lett. **22**, 2709–2712, https://doi.org/10.1029/95GL02781 (1995).

[11]V. M. Vasyliunas, "A survey of low-energy electrons in the evening sector of the magnetosphere with OGO 1 and OGO 3," J. Geophys. Res. **73**, 2839–2884, https://doi.org/10.1029/JA073i009p02839 (1968).

[12]M. A. Hellberg, R. L. Mace, T. K. Baluku, I. Kourakis, and N. S. Saini, "Comment on 'Mathematical and physical aspects of Kappa velocity distribution' [Phys. Plasmas **14**, 110702 (2007)]," Phys. Plasmas **16**, 094701 (2009).

[13]C. Tsallis, "Possible generalization of Boltzmann-Gibbs statistics," J. Stat. Phys. **52**, 479–487 (1988).

[14]F. Verheest, "Ambiguities in the Tsallis description of non-thermal plasma species," J. Plasma Phys. **79**, 1031–1034 (2013).

[15]H. Ur-Rehman and S. Mahmood, "Dust-ion acoustic cnoidal waves and associated nonlinear ion flux in a nonthermal dusty plasma," Astrophys. Space Sci. **361**, 292 (2016).

[16]N. S. Saini and P. Sethi, "Dust ion-acoustic cnoidal waves in a plasma with two temperature superthermal electrons," Phys. Plasmas **23**, 103702 (2016).

[17]R. E. Tolba, W. M. Moslem, A. A. Elsadany, N. A. El-Bedwehy, and S. K. El-Labany, "Development of cnoidal waves in positively charged dusty plasmas," IEEE Trans. Plasma Sci. **45**, 2552–2560 (2017).

[18]K. Singh, Y. Ghai, N. Kaur, and N. S. Saini, "Effect of polarization force on dust-acoustic cnoidal waves in dusty plasma," Eur. Phys. J. D **72**, 160 (2018).

[19]N. Kaur, M. Singh, R. Kohli, and N. S. Saini, "Effect of ion beam on low-frequency cnoidal waves in a non-Maxwellian dusty plasma," IEEE Trans. Plasma Sci. **46**, 768–774 (2018).

[20]E. F. El-Shamy and M. M. Selim, "Dust-acoustic periodic travelling waves in a magnetized dusty plasma with trapped ions and nonthermal electrons in astrophysical situations: Oblique excitations," Astrophys. Space Sci. **367**, 100 (2022).

[21]C. P. Olivier and F. Verheest, "A new reductive perturbation formalism for ion acoustic cnoidal waves," J. Plasma Phys. **88**, 905880601 (2022).

[22]A. E. Dubinov, "On one widely-spread inaccuracy and its elimination in the theories of nonlinear electrostatic waves in plasmas based on the Sagdeev's pseudopotential approach," Plasma Phys. Rep. **49**, 362–369 (2023).

[23]F. Verheest and C. P. Olivier, "Sagdeev pseudopotential analysis of nonlinear periodic ion-acoustic plasma waves," Phys. Plasmas **30**, 092306 (2023).

[24]F. Verheest and C. P. Olivier, "Nonlinear periodic ion-acoustic waves in non-thermal plasmas," Phys. Plasmas **31**, 032305 (2024).

[25]F. Verheest and S. R. Pillay, "Large amplitude dust-acoustic solitary waves and double layers in nonthermal plasmas," Phys. Plasmas **15**, 013703 (2008).

[26]F. Verheest and S. R. Pillay, "Dust-acoustic solitary structures in plasmas with nonthermal electrons and positive dust," Nonlin. Processes Geophys. **15**, 551–555 (2008).

[27]J. S. Pickett, J. R. Franz, J. D. Scudder, J. D. Menietti, D. A. Gurnett, G. B. Hospodarsky, R. M. Braunger, P. M. Kintner, and W. S. Kürth, "Plasma waves observed in the cusp turbulent boundary layer: An analysis of high time resolution wave and particle measurements from the Polar spacecraft," J. Geophys. Res. **106**(A9), 19081–19099, https://doi.org/10.1029/2000JA003012 (2001).

[28]O. R. Rufai, "Periodic low-frequency electric field structures in a magnetized non-thermal auroral plasma," Heliyon **5**, e01976 (2019).

[29]S. V. Singh, R. Rubia, S. Devanandhan, and G. S. Lakhina, "Nonlinear electrostatic waves in the auroral plasma," Phys. Scr. **95**, 075602 (2019).

[30]R. Z. Sagdeev, "Cooperative phenomena and shock waves in collisionless plasmas," in *Reviews of Plasma Physics*, edited by M. A. Leontovich (Consultants Bureau, New York, 1966), Vol. 4, pp. 23–91.